Reports

Molybdenum Disulfide in the Poorly Crystalline "Rag" Structure

Abstract. *Molybdenum disulfide has been prepared in an unusual poorly crystalline form, termed the "rag" structure, consisting of several stacked but highly folded and disordered S-Mo-S layers. This previously unknown structure demonstrates the flexible and macromolecular nature of the layered transition metal dichalcogenides. The determination of this structure provides a basis for understanding its highly broadened x-ray diffraction pattern and relatively low surface area, and is a starting point for optimizing the catalytic and surface properties of molybdenum disulfide.*

The layered transition metal dichalcogenides have found a wide variety of uses. Since before World War II, MoS_2 and WS_2 have been the basis for some of the most widely used hydrocarbon processing catalysts (*1*); MoS_2 has been used as a lubrication additive and TiS_2 as a cathode for lithium nonaqueous batteries (*2*). These applications arise in part from the highly anisotropic physical properties of these materials (*3*), which are due to their crystal structure. In this structure single layers of transition metals are sandwiched between two layers of close-packed chalcogen atoms. Within these layers the transition metal atoms are bound to six sulfur atoms which are arranged trigonally (MoS_2) or octahedrally (TiS_2) about the metal. Each sulfur atom bridges three transition metal atoms within the same layer, forming the only strong bonds in the structure. Because of these strong intralayer forces, the layers can be viewed as two-dimensional macromolecules which stack, bound only by van der Waals forces, to form three-dimensional crystals (*4*). Alkali metals and organic bases can be inserted (intercalated) between these layers (*5*).

We report here another manifestation of the anisotropic and macromolecular nature of the transition metal dichalcogenides: the preparation and characterization of MoS_2 in a new morphological structure termed the "rag" structure (Fig. 1). The rag depicted consists of several stacked but highly folded and disordered MoS_2 layers. Although only

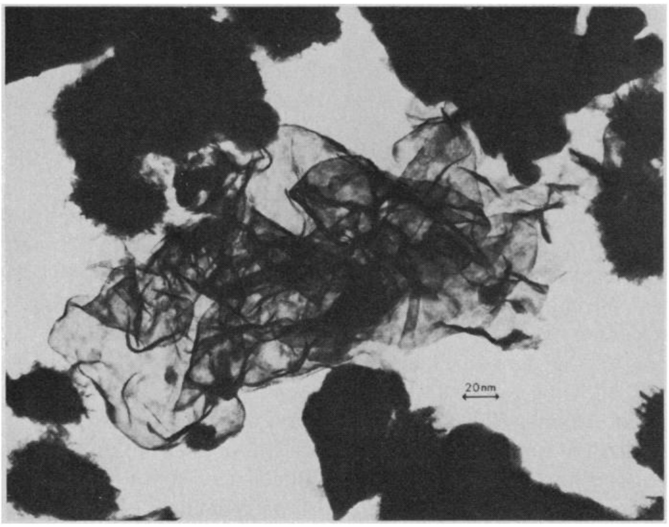

Fig. 1 (top left). The rag structure of MoS_2, a highly folded but disordered stacking pattern. Such a structure clearly shows the strong tendency for growth within the layers but a weak tendency for the layers to stack.

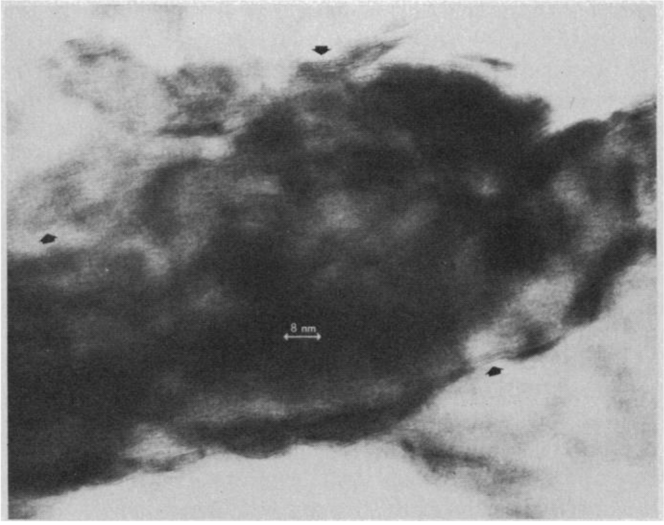

Fig. 2 (top right). The (002) planes of the MoS_2 within the rag structure. Arrows indicate ordered areas giving a 6.1-Å repeat. Larger areas in between appear to be completely disordered.

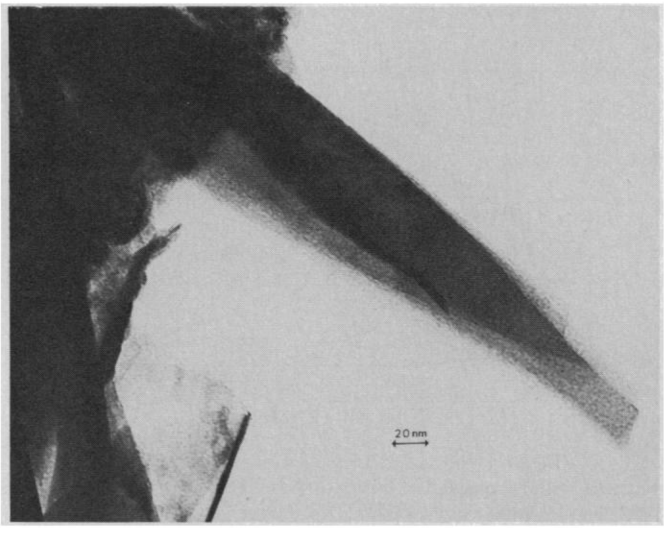

Fig. 3 (bottom right). A rolled sheet of MoS_2 (center and right) and a sheet folded back on itself. Rolled sheets give the appearance of "crystalline" needles at lower magnification.

0036-8075/79/0316-1105$00.50/0

20 to 30 Å thick in the stack direction, the layers extend several thousand angstroms perpendicular to the stack direction. By varying the conditions of preparation, one can vary the number of stacks and the dimensions of the layers as indicated below. We have reported the remarkable flexibility of the layers in TiS_2 as exhibited during the intercalation of lithium into single crystals (*6*). The existence of the rag structure in MoS_2 further demonstrates the flexibility and stability of the dichalcogenide layers.

The MoS_2 rag structure is prepared by the chemical precipitation of an intermediate amorphous MoS_2 phase at room temperature (*7*). The addition of 10 mmole of $MoCl_4$ (Ventron) and 20 mmole of Li_2S (Ventron) to 30 ml of tetrahydrofuron (THF), with stirring, produces a fine black solid, which on filtration and drying contains 70 percent (by weight) MoS_2. Repeated washings in THF remove by-product LiCl, and the remaining solvent is removed by heating at 100°C in a vacuum. The resulting material is amorphous MoS_2, which upon further heating to 400°C in a thermogravimetric analyzer in N_2 lost no more than 4 percent (by weight) and at this point had the stoichiometry $MoS_{2.0}$. This heat treatment produced a poorly crystalline MoS_2 having the layered MoS_2 molybdenite crystal structure. By varying the heating time and temperature, one can vary the stack number (the number of individual layers of trigonal, prismatically coordinated MoS_2 layers). For example, we prepared the material shown in Fig. 1 by heating several grams of amorphous MoS_2 for 2 hours at 400°C in a stream of H_2 mixed with 15 percent H_2S. This report will deal only with the structure of the poorly crystalline MoS_2, material consisting mostly of rags containing at least two layers and giving rise to a well-defined 002 x-ray reflection. The absence of this reflection in the x-ray diffraction pattern of the amorphous MoS_2 indicates that the rags, if present at all, are mostly individual layers. It is also possible that amorphous MoS_2 has a completely different structure (*8*).

Table 1. Electron diffraction data ($\pm$ 0.03 Å).

$d_{obs.}$	$d_{calc.}$	$hk\ell$
2.74	2.74	100
1.58	1.58	110
1.36	1.36	201

We used a high-resolution electron microscope (Philips EM-300) with a resolution of at least 2.5 Å. The sulfide samples were ground with a mullite mortar and pestle and were ultrasonically dispersed in heptane. A drop of the suspension was air-dried on a carbon-coated electron microscope grid for examination in the electron microscope. We calibrated the magnifications, using a replica of a diffraction grating as the low-magnification standard and the lattice image of the 3.44-Å spacing of the (002) planes in graphitized carbon black as the high-magnification standard. Under these conditions lattice images in the MoS_2 rags were often seen.

We can see in Fig. 2 (002) planes giving a repeat distance of 6.2 ± 0.2 Å, which is consistent with the MoS_2 *c*-axis repeat. The sheets were often rolled in cylinders (Fig. 3), which at lower magnification gave the appearance of needles. We can also see (lower left corner of Fig. 3) what appears to be a single sheet folded back on itself. Large areas of highly folded MoS_2 are seen in all the figures that we have examined, showing very little evidence of ordered lattice images.

Raglike MoS_2 gave rise to smooth electron diffraction rings with strong maxima corresponding to interplanar or *d*-spacings for the 100 and 110 planes of MoS_2; 00ℓ maxima were rarely seen, an indication that the layers were lying flat, and a faint 201 was seen in some cases. The data in Table 1 are in agreement with the x-ray diffraction data described below.

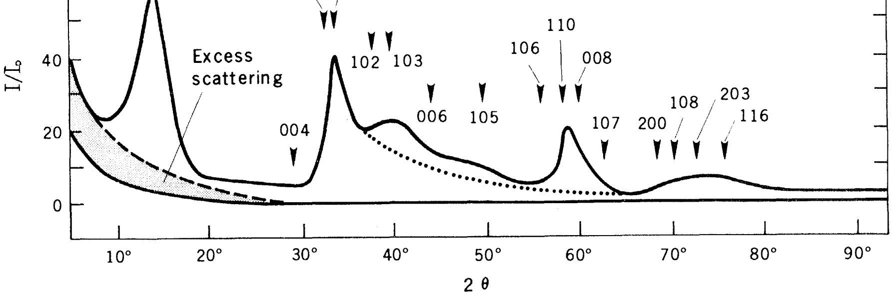

Fig. 4. Crystalline peaks of poorly crystalline or rag MoS_2. The intensity (I/I_0) is plotted as a function of scattering angle (2θ).

We obtained x-ray powder diffraction patterns by lightly packing samples of the black powders into normal Philips x-ray powder sample holders used on a standard Philips x-ray powder diffractometer (CuK_α radiation). A scan speed of 1/8° per minute was used with a chart speed adjusted to record a scattering angle (2θ) of 1° in 1 inch. The base line was adjusted to read zero with the x-ray shutter closed, and the scale factor and time constant were adjusted to give a smooth curve with the largest maximum just on scale (typically a scale factor of × 250 and a time constant of 5 seconds were used). Scans were generally made to over $2\theta = 100°$ (the data collection time was approximately 14 hours). Figure 4 illustrates a typical scan that is characteristic of poorly crystalline layered disulfides; it is similar to the scan reported by Wildervanck and Jellinek for MoS_2 produced by the decomposition of MoS_3 (*9*). It exhibits a strong 002 maximum in the low-angle region and a broad envelope beginning approximately at $2\theta = 30°$ and continuing out to above $2\theta = 60°$. This envelope contains the 100, 101, 102, 103, 006, 105, 106, 110, and 008 reflections with well-defined maxima appearing for the 100, 103, and 110 reflections. The maximum at 103 indicates that the 2H (two-layer hexagonal) molybdenite stacking sequence is retained in some crystallites.

Line-broadening analyses of the well-defined maxima carried out in the standard manner (*10*) resulted in an average x-ray crystallite size of about 28 Å in the *c*-direction (approximately four MoS_2 layers) and 78 Å in the *a*-direction. Crystallites of these dimensions should have surface areas of several hundred square meters per gram, but the actual N_2 BET (Brunauer, Emmett, and Teller) measurements were approximately 50 m²/g. This can be explained if we realize that x-ray measurements represent only the average unstrained repeat distances (order length) within the rags. For example, in Fig. 2 we can see *c*-axis stackings of 10, 11, and 5 layers (indicated by arrows), all of which are longer than the x-ray measurement of 4 layers. Moreover, the *a*-axis dimensions observed with the transmission electron microscope were of the order of several thousand angstroms. If we assume that the rags are infinite in extent, the surface area will depend only on the basal plane area and thus on the number of stacked sheets, which we assume are double layers as in 2H molybdenite on the basis of the results discussed above:

$$\text{Surface area} = \text{m}^2/\text{g} = 327/n$$

where n is the number of stacked sheets or rags. For five to ten stacks this yields calculated surface areas in the range of about 33 to 66 m^2/g, in good agreement with the observed value but indicating that there is also a greater degree of stacking than indicated by the x-ray order length in the c-direction.

The asymmetric shape of the 100 envelope (as indicated in Fig. 4) is characteristic of random layer lattice structures (*11*), in which the layers are displaced randomly with respect to one another like a spread deck of cards. They are stacked almost normally, although the position of the 002 reflection is displaced slightly to lower angles; this displacement is presumably due to imperfect stacking, as has been described for graphite (*12*). When a mixed reflection such as the 103 reflection appears, its line width indicates that the two-layer molybdenite stacking sequence is maintained for at least two stacks as might be expected. We also observed that pressing the "poorly crystalline" MoS_2 in a laboratory press at approximately 1000 atm significantly increased the sharpness of the x-ray reflections, presumably improving the stacking of the rags. There is considerable non-Bragg scattering present at low angles (Fig. 4). This may be due to uncorrelated single layers and the pore structure that they generate by randomly folding and connecting with other sheets. All of the above observations are consistent with the stacking and folding of individual MoS_2 layers to form a highly disordered, poorly crystalline MoS_2.

This study demonstrates that the rag morphology in poorly crystalline MoS_2 arises from the two-dimensional macromolecular nature of the layered MoS_2 crystal structure. We believe that the anisotropic properties of MoS_2 rags will have important implications in catalysis and surface chemistry (*8*). The structure of amorphous MoS_2 and how this is related to the crystallization and growth of MoS_2 in the rag structure are still open questions.

R. R. CHIANELLI
E. B. PRESTRIDGE
T. A. PECORARO
J. P. DENEUFVILLE
Corporate Research Laboratories,
Exxon Research and Engineering
Company, Linden, New Jersey 07036

References

1. O. Weisser and S. Landa, *Sulfide Catalysts, Their Properties and Applications* (Pergamon, New York, 1973).
2. M. S. Whittingham, *Science* **192**, 1126 (1976); *Prog. Solid State Chem.* **12**, 1 (1977).
3. F. R. Gamble, F. J. DiSalvo, R. A. Klemm, T. H. Geballe, *Science* **168**, 568 (1970).
4. R. Schollhorn, E. Sick, A. Serf, *Mater. Res. Bull.* **10**, 1005 (1975).
5. F. R. Gamble, J. H. Osiecki, M. Cais, R. Pisharody, F. J. DiSalvo, T. H. Geballe, *Science* **174**, 493 (1971).
6. R. R. Chianelli, *J. Cryst. Growth* **34**, 239 (1976).
7. ——— and M. B. Dines, *Inorg. Chem.* **17**, 2758 (1978).
8. R. R. Chianelli, E. B. Prestridge, T. A. Pecoraro, J. P. DeNeufville, in preparation.
9. A. Wildervanck and F. Jellinek, *Z. Anorg. Allg. Chem.* **328**, 309 (1964).
10. H. P. Klug and L. E. Alexander, *X-ray Diffraction Procedures for Polycrystalline and Amorphous Materials* (Wiley, New York, 1954).
11. A. Guinier, *X-ray Diffraction in Crystals, Imperfect Crystals, and Amorphous Bodies* (Freeman, San Francisco, 1963).
12. S. Ergun, *Carbon* **3**, 211 (1968).

3 October 1978; revised 8 December 1978

Defects of Bile Acid Synthesis in Zellweger's Syndrome

Abstract. *Abnormal mitochondrial structure and function have been documented in patients with Zellweger's syndrome (cerebrohepatorenal syndrome). In vitro studies have suggested that the formation of C_{24} bile acids (chenodeoxycholic acid and cholic acid) from C_{27} cholesterol requires mitochondrial oxidative cleavage of the terminal three carbons of the side chain. Therefore, three patients with Zellweger's syndrome were examined for the presence of mitochondrial defects in bile acid synthesis. All three excreted excessive amounts of 3α,7α-dihydroxy-5β-cholestan-26-oic acid, 3α,7α,12α-trihydroxy-5β-cholestan-26-oic acid, and 3α,7α,12α,24ξ-tetrahydroxy-5β-cholestan-26-oic acid (varanic acid), precursors of chenodeoxycholic acid and cholic acid that have undergone only partial side chain oxidation. These findings give added support to the role of mitochondrial oxidative side chain cleavage in the overall scheme of bile acid synthesis.*

Bile acids are synthesized from cholesterol in the liver and are important for the solubilization of cholesterol in bile and fat in the intestinal tract as well as being an excretory pathway for cholesterol. The synthesis of bile acids has been extensively studied in vitro, and it is thought that the initial steps of hydroxylation and rearrangement of the ring system of cholesterol take place in the endoplasmic reticulum and that side chain oxidation and cleavage take place in the mitochondria (*1*).

In 1964, Bowen *et al.* (*2*) described an autosomal recessive disease (Zellweger's syndrome) characterized by severe hypotonia, growth and mental retardation, renal cortical cysts, and liver dysfunction. Patients with this syndrome also have severe mitochondrial abnormalities (*3*). Thus, Zellweger's syndrome appears to be a unique "experiment of nature" in which the role of the mitochondria in bile acid synthesis could be assessed in vivo.

We studied three patients with typical features of this syndrome (*4*). Liver biopsies, obtained from two patients, showed abnormalities of the mitochondria consisting of disarrangement and twisting of the cristae. In addition, no peroxisomes could be identified. These electron microscopic findings are similar to those previously reported in Zellweger's syndrome (*3*).

Samples of urine from these three pa-

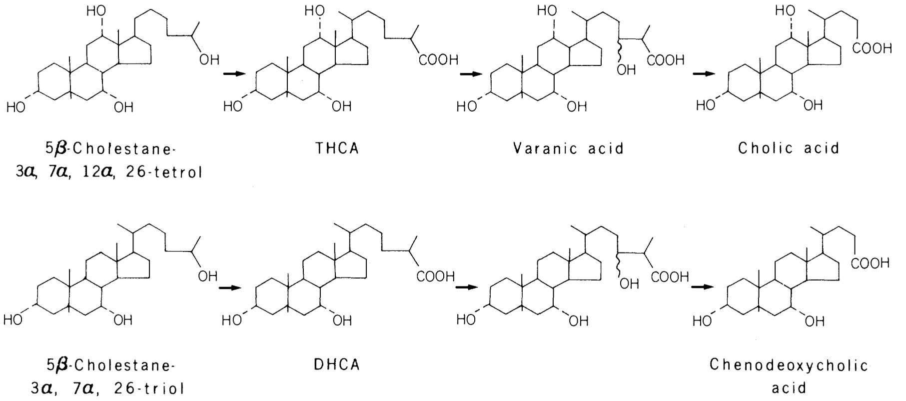

Fig. 1. Side chain oxidation in the synthesis of cholic acid from 5β-cholestane-3α,7α,12α,26-tetrol and chenodeoxycholic from 5β-cholestane-3α,7α,26-triol, respectively. Abbreviations: THCA, 3α,7α,12α-trihydroxy-5β-cholestan-26-oic acid; DHCA, 3α,7α-dihydroxy-5β-cholestan-26-oic acid; varanic acid, 3α,7α,12α,24ξ-tetrahydroxy-5β-cholestan-26-oic acid.